

Scattering of a Klein-Gordon particle by an Exponential-Tanh Potential

SALAZAR ANGEL^{1,*} AND POTOSI QURAY^{2,**}

¹ School of Physical Sciences and Nanotechnology, Yachay Tech University, Urcuquí-Ecuador

² School of Physical Sciences and Nanotechnology, Yachay Tech University, Urcuquí-Ecuador

* angel.salazar@yachaytech.edu.ec

** quray.potosi@yachaytech.edu.ec

Compiled December 8, 2025

We investigate the phenomenon of superradiance, the amplification of a reflected wave, within the scattering of a spin 0 Klein-Gordon particle from an asymmetric exponential-tanh potential, $V(x) = ae^{b\tanh(cx)}$. The potential's asymptotic structure creates distinct left and right regions with constant effective potentials, enabling a clear analysis of scattering channels. We derive the condition for superradiance, which occurs when the transmitted mode carries negative Klein-Gordon flux, leading to a reflection coefficient $R(E) > 1$. This condition defines the superradiant window $V_R - m < E < V_R + m$ with $E < V_R$, where V_R is the right asymptotic potential value. Using the numerically stable Riccati log-derivative method, we compute the energy-dependent reflection and transmission coefficients for representative parameter sets. Our results confirm the existence of three distinct scattering regimes: a superradiant amplification region for $E < V_R - m$, a total-reflection (evanescent) plateau for $V_R - m < E < V_R + m$, and a high-energy transparent regime for $E > V_R + m$. We demonstrate that both the height (a , b) and steepness (c) of the potential significantly enhance the superradiant effect, with taller and sharper barriers producing stronger amplification. This work establishes the exponential-tanh potential as a versatile model for studying relativistic scattering phenomena and provides a clear numerical demonstration of superradiance rooted in the Klein paradox for bosonic fields.

1. INTRODUCTION

The study of quantum systems under the influence of various potential barriers is a cornerstone of quantum mechanics and has far-reaching implications in understanding the behavior of particles in diverse physical scenarios. Among these, the Klein-Gordon equation, a relativistic wave equation that describes spin-0 particles, plays a pivotal role in quantum field theory and has been instrumental in elucidating the properties of fundamental particles.

The phenomenon of superradiance, first predicted by Zel'dovich in the context of rotating black holes [1], refers to the process by which a system can extract energy from a rotating black hole or other coherent sources, leading to an amplification of waves. This intriguing effect has since been explored in various physical systems, including quantum mechanical systems with specific potential barriers that mimic certain aspects of black hole physics [2].

In this paper, we focus on the superradiance phenomenon within the framework of the Klein-Gordon equation, employing a novel potential barrier given by $V(x) = ae^{b\tanh(cx)}$. This potential is of particular interest due to its non-linear and non-analytic nature, which introduces complexities not present in more traditional potential forms.

Our analysis will involve solving the Klein-Gordon equation with the specified potential and examining the conditions under which superradiance can occur. We will explore the dependence of superradiance on various parameters of the potential, including the amplitude a , the steepness b , and the characteristic scale c . Additionally, we will investigate the implications of these findings for the stability and dynamics of the system, as well as their potential connections to other areas of physics, such as condensed matter systems and quantum information theory.

The structure of this paper is as follows: In Section II, we present the theory and mathematical formulation of the problem. Section III is dedicated to the numerical and analytical methods employed to solve the equation and analyze the superradiance phenomenon. Our results are presented in Section IV, where we discuss the behavior of the system under different parameter regimes. Finally, in Section V, we summarize our findings and discuss potential avenues for future research.

² <http://dx.doi.org/10.1364/ao.XX.XXXXXX>

³

2. THEORY

This section presents the theoretical framework for analyzing the scattering of a spin 0 particle, described by the Klein-Gordon equation, from an asymmetric exponential tanh potential. We derive the conditions under which the phenomenon of superradiance, the amplification of a reflected wave occurs, and define the numerical setup used for its investigation.

A. Klein-Gordon Equation

The dynamics of a relativistic spin 0 particle of mass m are governed by the Klein-Gordon equation. In natural units ($\hbar = c = 1$) and for a static potential $V(x)$, the stationary one-dimensional equation is [3]:

$$\frac{d^2\phi(x)}{dx^2} + \left[(E - V(x))^2 - m^2 \right] \phi(x) = 0, \quad (1)$$

where E is the energy of the particle and $\phi(x)$ is the wave function. Equation Eq. (1) is the fundamental equation to be solved for the scattering problem.

B. The Exponential-Tanh Potential and its Asymptotic Structure

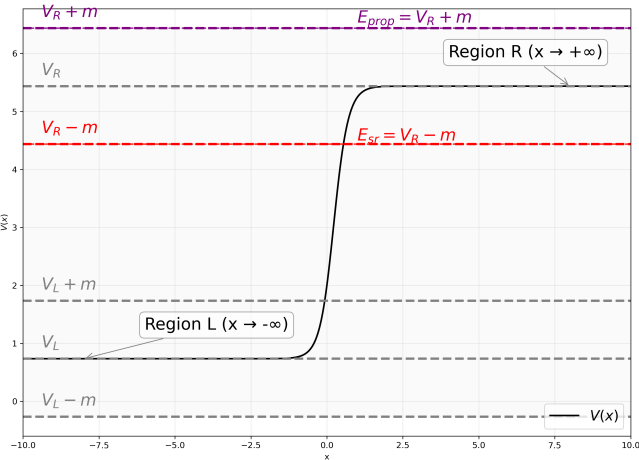


Fig. 1. Asymptotic structure of the exponential tanh potential $V(x) = ae^b \tanh(cx)$. The left region ($x \rightarrow -\infty$) approaches V_L , while the right region ($x \rightarrow +\infty$) approaches V_R . The dashed horizontal lines indicate the relativistic thresholds $V_{L,R} \pm m$, which determine the behavior of Klein-Gordon solutions: propagating modes exist when $(E - V_{L,R})^2 > m^2$, whereas the interval $V_R - m < E < V_R + m$ corresponds to the superradiant regime where the transmitted flux becomes negative.

We study the scattering for a specific asymmetric potential model:

$$V(x) = ae^b \tanh(cx), \quad (2)$$

where a , b , and c are real parameters controlling the amplitude, asymmetry, and steepness of the transition, respectively.

The key to understanding the scattering problem lies in the asymptotic behavior of the potential [4].

Using the limits $\lim_{x \rightarrow -\infty} \tanh(cx) = -1$ and $\lim_{x \rightarrow +\infty} \tanh(cx) = +1$, the potential approaches different constant values on the left and [5]:

$$V_L = \lim_{x \rightarrow -\infty} V(x) = ae^{-b}, \quad V_R = \lim_{x \rightarrow +\infty} V(x) = ae^b. \quad (3)$$

The asymmetry ($V_L \neq V_R$) is a crucial feature for the phenomena discussed later.

In these asymptotic regions where $V(x) \rightarrow V_{L,R}$, the Klein-Gordon equation Eq. (1) simplifies. Solutions take the plane-wave form $\phi(x) \sim e^{\pm ik_{L,R}x}$, with wave numbers given by:

$$k_{L,R} = \sqrt{(E - V_{L,R})^2 - m^2}. \quad (4)$$

A given asymptotic region supports propagating modes (real $k_{L,R}$) if $(E - V_{L,R})^2 > m^2$; otherwise, the solutions are evanescent, indicating a tunneling regime.

C. Scattering Channels and Conserved Current

Consider an incident plane wave of unit amplitude coming from the left ($x \rightarrow -\infty$) [6]. The asymptotic scattering states are:

$$\phi(x) \sim e^{ik_L x} + R e^{-ik_L x}, \quad \text{for } x \rightarrow -\infty, \quad (5)$$

$$\phi(x) \sim T e^{ik_R x}, \quad \text{for } x \rightarrow +\infty, \quad (6)$$

where R and T are the reflection and transmission amplitudes, respectively.

For the stationary Klein-Gordon equation, the conserved probability current is:

$$j(x) = \frac{i}{2} (\phi^* \partial_x \phi - \phi \partial_x \phi^*). \quad (7)$$

For a plane wave $e^{\pm ikx}$, the current is $j = \mp |k|$. Flux conservation implies that the incoming current must equal the sum of the reflected and transmitted currents. A central relativistic feature is that the sign of j for a propagating mode is determined by the sign of the group velocity, $v_g = k/(E - V)$, which can be opposite to the sign of k if $E - V < 0$ [3]. This allows for modes with positive momentum ($k > 0$) to carry negative flux ($j < 0$).

D. Theory of Superradiance

Superradiance in this context refers to the amplification of the reflected wave, such that the reflection coefficient $R(E) = |j_{\text{ref}}| / |j_{\text{in}}|$ exceeds unity [2]. This is permitted by flux conservation when the transmitted mode carries negative flux [7].

D.1. Condition for Superradiance

From Eq. (7) and Eq. (4), the transmitted Klein-Gordon flux associated with the right-going wave in Eq. (6) is proportional to the product

$$j_{\text{trans}} \propto k_R (E - V_R), \quad (8)$$

where k_R is the asymptotic wave number on the right. With the usual convention $k_R > 0$, the sign of the transmitted flux is determined entirely by the sign of $(E - V_R)$.

Superradiance requires that:

- the right region supports a propagating mode,

$$(E - V_R)^2 > m^2 \implies k_R \in \mathbb{R}, \quad (9)$$

- the transmitted flux is negative,

$$E - V_R < 0. \quad (10)$$

Combining these two conditions yields the inequality

$$E < V_R - m, \quad (11)$$

which defines the superradiant regime on the right-hand side. In addition, the left region must support an incoming propagating wave,

$$(E - V_L)^2 > m^2, \quad (12)$$

so that a well-defined scattering process exists.

Within the energy range where both asymptotic regions are propagating and Eq. (11) holds, the transmitted flux satisfies $j_{\text{trans}} < 0$, while the incoming flux $j_{\text{in}} > 0$. Flux conservation,

$$j_{\text{in}} = j_{\text{ref}} + j_{\text{trans}}, \quad (13)$$

then implies that the magnitude of the reflected flux exceeds that of the incident flux, $|j_{\text{ref}}| > |j_{\text{in}}|$, which is equivalent to

$$R(E) > 1. \quad (14)$$

This is the defining signature of Klein superradiance [8]

D.2. Connection to the Klein Paradox and the Exponential-Tanh Potential

This superradiant mechanism is directly related to the Klein paradox for bosonic fields [9]. It occurs because the effective energy for propagation on the right, $(E - V_R)$, is negative, flipping the sign of the group velocity relative to the momentum. The transmitted particle thus behaves as having negative energy relative to the potential height, leading to a negative probability flux.

The exponential-tanh potential Eq. (2) is ideally suited to study this effect. Its inherent asymmetry ($V_R > V_L$) is essential, as a symmetric barrier cannot produce a transmitted mode with reversed flux under the same incident energy. Furthermore, the parameter c controls the sharpness of the step. A larger c creates a more abrupt transition, increasing the wave number mismatch (k_L vs. k_R) and typically enhancing the superradiant amplification by reducing tunneling that would otherwise suppress the effect [10].

E. Numerical Setup and Reference Parameters

To provide concrete context for the subsequent analysis, we define a reference set of parameters for the potential and the numerical integration domain.

We choose particle mass $m = 1.0$ and potential parameters:

$$a = 2.0, \quad b = 1.0, \quad c = 2.0. \quad (15)$$

From Eq. (3), this yields the asymptotic values $V_L \approx 0.736$ and $V_R \approx 5.437$. The potential, plotted in Fig. 2, thus forms a smooth, asymmetric step barrier.

For the numerical solution of Eq. Eq. (1) via the Riccati log-derivative method, the spatial domain is truncated to $x \in [X_{\min}, X_{\max}] = [-10.0, 10.0]$. This interval is sufficiently large for the potential to reach its asymptotic values at the boundaries, ensuring the scattering boundary conditions Eq. (5) and Eq. (6) are valid. The domain is discretized into $N_{\text{steps}} = 6000$ points, providing adequate resolution for the rapid variation of the potential near $x = 0$ where $\tanh(cx)$ transitions.

3. RICCATI LOG-DERIVATIVE METHOD (RLM)

Using the Klein-Gordon equation Eq. (1) we define the local relativistic wave number as

$$k^2(x) = (E - V(x))^2 - m^2, \quad (16)$$

Eq. (1) becomes formally similar to a Schrödinger-type wave equation, but with a nonlinear dependence on the potential.

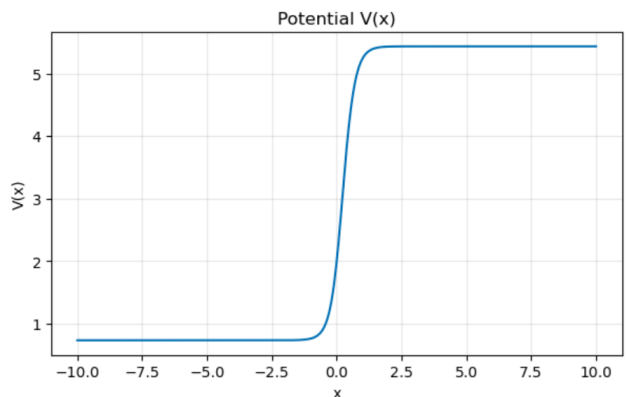


Fig. 2. Exponential-tanh potential $V(x) = ae^{bx} \tanh(cx)$ for the reference parameters in Eq. (15). The potential interpolates smoothly between the asymptotic values V_L and V_R , forming an asymmetric step-like barrier. The dashed lines indicate the asymptotic levels.

Direct numerical integration of Eq. Eq. (1) is typically unstable because the independent solutions contain exponential growth and decay in classically forbidden regions.

To overcome these instabilities, we follow the approach introduced by Johnson [11] and reviewed by Razavy [12], and rewrite the second-order KG equation in terms of the *logarithmic derivative*

$$y(x) = \frac{\phi'(x)}{\phi(x)}. \quad (17)$$

Differentiating this expression and substituting Eq. Eq. (1) yields the first-order nonlinear Riccati equation

$$y'(x) = -k^2(x) - y^2(x), \quad (18)$$

which is numerically far more stable than direct integration of the wavefunction $\phi(x)$, as $y(x)$ is invariant under any overall normalization of $\phi(x)$. This property makes the Riccati method particularly suitable for relativistic scattering problems where exponential amplification or suppression of the wavefunction is expected [13].

A. Boundary Condition and Backward Integration

In the right asymptotic region $x \rightarrow +\infty$, the potential approaches a constant value V_R , and the Klein-Gordon equation admits plane-wave solutions. Imposing the physical boundary condition of a purely outgoing wave,

$$\phi(x) \sim e^{ik_R x}, \quad k_R = \sqrt{(E - V_R)^2 - m^2}, \quad (19)$$

the logarithmic derivative satisfies

$$y(x_R) = ik_R. \quad (20)$$

This condition serves as the starting point for integrating the Riccati equation Eq. (18) from a sufficiently large x_R back toward the left asymptotic region x_L . The integration is carried out using a fourth-order Runge-Kutta method with small step size, following the prescription of Johnson [11]. To avoid numerical overflow, the Riccati variable is capped whenever $|y(x)|$ exceeds a large threshold.

185 **B. Extraction of the Reflection Coefficient**

186 In the left asymptotic region the solution takes the form

$$\phi(x) = e^{ik_L x} + Re^{-ik_L x}, \quad k_L = \sqrt{(E - V_L)^2 - m^2}, \quad (21)$$

187 where R is the complex reflection amplitude. Taking the logarithmic derivative of Eq. (21) and evaluating at $x = x_L$, one
188 obtains after algebraic manipulation
189

$$R = e^{2ik_L x_L} \frac{ik_L - y(x_L)}{ik_L + y(x_L)}. \quad (22)$$

190 The physical reflection coefficient is then

$$R(E) = |R|^2. \quad (23)$$

191 **C. Transmission and Flux Conservation**

192 For real static potentials, the Klein–Gordon current is conserved.
193 Whenever both asymptotic regions allow propagating states, the
194 transmission coefficient follows from

$$T(E) = 1 - R(E). \quad (24)$$

195 In the superradiant regime, where the group velocity on the right
196 is opposite to the momentum, the flux $T(E)$ becomes negative
197 and the reflection exceeds unity, a phenomenon well understood
198 in relativistic scattering theory.

199 **D. Advantages of the Riccati Method**

200 The Riccati Log–Derivative Method provides excellent numerical
201 stability because it removes the exponentially growing and
202 decaying components of the wavefunction from the computation,
203 evolving only the ratio ϕ'/ϕ . This makes it particularly
204 effective in relativistic tunneling and superradiant scattering,
205 as discussed in Refs. [11, 12]. The method also yields immediate
206 access to the reflection amplitude through the closed-form
207 expression Eq. (22), avoiding the need to propagate linearly in-
208 dependent solutions or to match absolute wavefunction values.

209 **4. RESULTS**

210 We present the reflection and transmission coefficients for two
211 distinct parameter sets to illustrate the effect of barrier shape.

212 **A. Case I: Moderate Barrier ($a = 2.0, b = 2.0, c = 3.0$)**

213 Figure 3 displays the scattering coefficients. Here, $V_R \approx 14.78$.

- 214 • **Superradiance ($E < 13.78$):** We observe $R(E) > 1$ and
215 $T(E) < 0$. The reflected flux is amplified due to the negative
216 flux of the transmitted mode.
- 217 • **Evanescence Plateau ($13.78 < E < 15.78$):** The region $V_R -$
218 $m < E < V_R + m$ acts as a total reflection barrier ($R = 1, T = 0$).
- 219 • **Transparency ($E > 15.78$):** At high energies, the potential
220 becomes transparent.

222 **B. Case II: Steep Barrier ($a = 5.0, b = 1.0, c = 6.0$)**

223 Figure 4 shows the results for a sharper potential with $V_R \approx$
224 13.59. The superradiance occurs for $E < 12.59$. Notably, the peak
225 amplification is significantly higher ($R \approx 3.3$) compared to Case
226 I. The sharp transition ($c = 6.0$) enhances the mode mismatch,
227 driving stronger amplification.

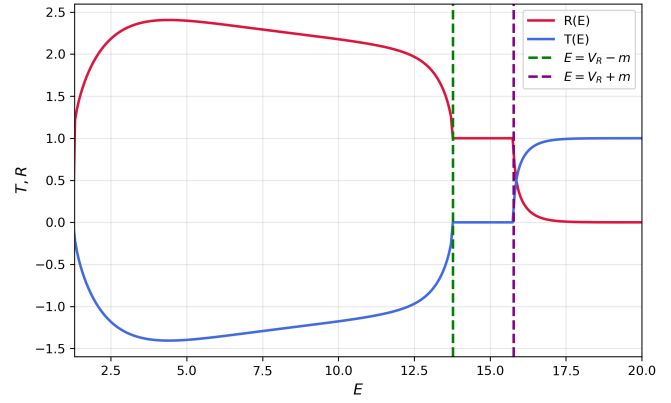


Fig. 3. Reflection and transmission coefficients for Case I ($a = 2, b = 2, c = 3$). Superradiance is visible for $E < V_R - m$, followed by a plateau of total reflection.

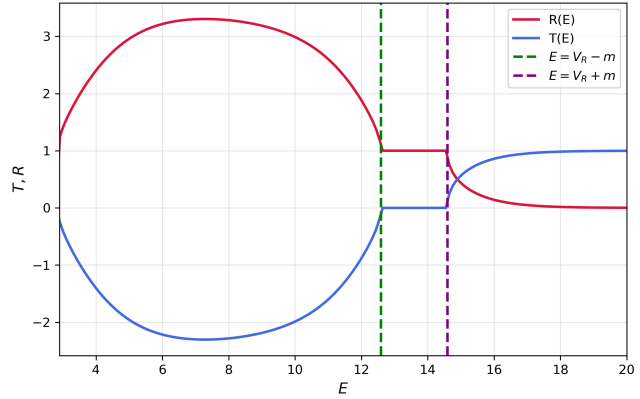


Fig. 4. Reflection and transmission coefficients for Case II ($a = 5, b = 1, c = 6$). The steeper potential produces stronger superradiant amplification.

228 **5. DISCUSSION**

229 The two parameter sets analyzed in this work provide a clear
230 illustration of how the structure of the exponential–tanh potential
231 influences relativistic scattering in the Klein–Gordon equation.
232 Although both cases exhibit the same qualitative scattering
233 regimes: superradiance, an evanescent plateau, and high en-
234 ergy transparency. The magnitude and location of these effects
235 depend sensitively on the potential height and steepness.

236 **A. Superradiance and the role of the right asymptotic potential**

237 For the Klein–Gordon equation with a vector potential, super-
238 radiant amplification occurs when the right asymptotic region
239 supports propagating modes with reversed flux [14]. This re-
240 quires

$$(E - V_R)^2 > m^2 \quad \text{and} \quad E - V_R < 0,$$

241 which together define the superradiant window

$$V_R - m < E < V_R + m.$$

242 where both the left and right regions support propagating solu-
243 tions, but the group velocity of the transmitted mode is opposite

244 in sign to its momentum. This reversed flux condition produces
 245 $R(E) > 1$ and $T(E) < 0$, features that are present in both numer-
 246 ical experiments.

247 The height of the right asymptotic potential, $V_R = ae^b$, de-
 248 termines how far the superradiant window is shifted along the
 249 energy axis. In Case I this threshold lies near $E \approx 13.8$, while in
 250 Case II it occurs around $E \approx 12.6$. Even though these values are
 251 numerically close, the resulting scattering curves behave differ-
 252 ently because the barriers have different steepness and overall
 253 profiles.

254 **B. Effect of barrier height**

255 A comparison between the two cases shows that the magnitude
 256 of superradiant amplification increases significantly with the
 257 height of the potential. In Case I the reflection coefficient peaks
 258 around $R \approx 2.4$, whereas in Case II it reaches values $R \approx 3.3$.
 259 This enhancement is expected: a larger potential contrast in-
 260 creases the mismatch between the asymptotic wave numbers k_L
 261 and k_R , effectively strengthening the energy extraction mecha-
 262 nism that underlies Klein superradiance.

263 The transmission coefficient exhibits a correspondingly larger
 264 negative minimum in Case II, again consistent with stronger
 265 amplification of the reflected mode.

266 **C. Effect of barrier steepness**

267 The steepness parameter c controls how rapidly the potential
 268 transitions between its left and right asymptotic values [15].
 269 Larger values of c produce sharper gradients, which enhance
 270 reflection and amplify the superradiant response. This trend is
 271 visible when comparing Case I ($c = 3$) with Case II ($c = 6$): the
 272 broader and flatter superradiant peak of Case I contrasts with
 273 the narrower but stronger peak observed in Case II.

274 A sharper barrier also leads to more pronounced curvature in
 275 $T(E)$ below the superradiant threshold, reflecting the stronger
 276 mode coupling induced by the rapid spatial variation of $V(x)$.

277 **D. Evanescent plateau and re-emergence of transmission**

278 Both simulations exhibit a region of complete reflection,

$$V_R - m < E < V_R + m,$$

279 where the transmitted mode becomes evanescent and the group
 280 velocity vanishes [16]. The numerical results reproduce precisely
 281 the expected plateau $R(E) = 1$ and $T(E) = 0$, confirming the
 282 stability and accuracy of the Riccati Log-Derivative Method in
 283 this delicate regime.

284 For $E > V_R + m$, the right-hand region again supports propa-
 285 gating solutions. In both cases the reflection coefficient decreases
 286 rapidly and the transmission coefficient approaches unity, illus-
 287 trating the transparency of the potential at high energies. The
 288 decay is smoother in the shallower barrier (Case I) and more
 289 abrupt in the steeper and taller barrier of Case II.

290 These results confirm that the Riccati Log-Derivative Method
 291 is well suited to study relativistic scattering phenomena and
 292 faithfully reproduces the structural features of Klein superradi-
 293 ance for a wide range of potential profiles.

294 **E. Physical Interpretation: Pair Creation and Vacuum Instabil- 295 ity**

296 **F. Physical Interpretation**

297 The phenomenon of superradiance observed here, where
 298 $R(E) > 1$, admits a profound physical interpretation. Although
 299 our numerical results are derived from the single-particle wave

300 equation, a physically correct description of the underlying
 301 mechanism requires Quantum Field Theory (QFT). In the QFT
 302 framework, the condition for superradiance, $V_R > E + m$, im-
 303 plies that the potential step height $\Delta V \approx V_R$ exceeds the mass
 304 gap $2m$ required to create particle-antiparticle pairs [7].

305 **6. CONCLUSIONS**

306 In this work we analyzed Klein–Gordon scattering in the
 307 exponential–tanh potential using the Riccati Log–Derivative
 308 Method (RLM). The method proved to be numerically stable
 309 and well suited for relativistic scattering, accurately resolving
 310 the superradiant, evanescent, and propagating energy regimes
 311 across a wide range of potential parameters. We analyzed how
 312 the RLM correctly reproduced the condition for superradiance,
 313 yielding reflection coefficients exceeding unity and negative
 314 transmitted flux.

315 **REFERENCES**

- 316 1. I. ZEL'DOVICH, Sov. Physics-JETP **35**, 1085 (1972).
- 317 2. R. Penrose and R. M. Floyd, Nat. Phys. Sci. **229**, 177 (1971).
- 318 3. W. Greiner *et al.*, *Relativistic quantum mechanics*, vol. 3 (Springer, 319 1990).
- 320 4. J. D. Bjorken and S. D. Drell, (No Title) (1964).
- 321 5. G. Breit, Rev. Mod. Phys. **23**, 238 (1951).
- 322 6. L. Horwitz and Y. Lavie, Phys. Rev. D **26**, 819 (1982).
- 323 7. R. Brito, V. Cardoso, and P. Superradiance, Lect. Notes Phys **906**, 1 (2015).
- 324 8. A. Wachter, *Relativistic quantum mechanics*, vol. 422 (Springer, 325 2011).
- 326 9. C. A. Manogue, Ann. Phys. **181**, 261 (1988).
- 327 10. S. Endlich and R. Penco, J. High Energy Phys. **2017**, 1 (2017).
- 328 11. B. R. Johnson, J. Chem. Phys. **67**, 4086 (1977).
- 329 12. M. Razavy, *Quantum theory of tunneling* (World Scientific, 330 2013).
- 331 13. B. R. Johnson, The J. Chem. Phys. **69**, 4678 (1978).
- 332 14. M. Marinov and V. Popov, Fortschritte der Physik **25**, 373 (1977).
- 333 15. A. Rezaei Akbarieh and H. Motavali, Mod. Phys. Lett. A **23**, 3005 (2008).
- 334 16. M. Gross and S. Haroche, Phys. reports **93**, 301 (1982).